

Photoinduced Amino–Imino Tautomerism: An Infrared Study of 2-Amino-5-methylpyridine in a Low-Temperature Argon Matrix

Nobuyuki Akai,^{*,†} Takanori Harada,^{†,‡} Kei Shin-ya,[‡] Keiichi Ohno,[‡] and Misako Aida^{†,‡}

Center for Quantum Life Sciences, Hiroshima University, 1-3-1, Kagamiyama, Higashi-Hiroshima, Hiroshima 739-8530, Japan, and Department of Chemistry, Graduate School of Science, Hiroshima University, 1-3-1, Kagamiyama, Higashi-Hiroshima, Hiroshima 739-8526, Japan

Received: October 31, 2005; In Final Form: March 14, 2006

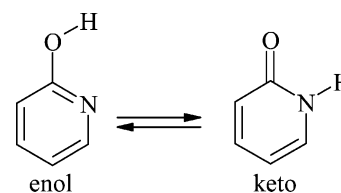
The photoreaction of 2-amino-5-methylpyridine was investigated by matrix-isolation infrared spectroscopy and DFT calculation. Photoinduced reversible amino ($\text{N}=\text{C}-\text{NH}_2$)–imino ($\text{NH}-\text{C}=\text{NH}$) tautomerism was found between 2-amino-5-methylpyridine and 5-methyl-2(1*H*)-pyridinimine; the amino tautomer changes to the imino tautomer by UV irradiation ($340 > \lambda \geq 300$ nm) and the reverse change occurs by longer-wavelength light irradiation ($420 > \lambda \geq 340$ nm). The results of the CASSCF calculation revealed that the amino–imino tautomerism proceeds in vibrational relaxation process from electronic excited state to the ground state. The IR spectra of 2-amino-5-methylpyridine in the T_1 state and 5-methyl-2-pyridinamino radical were also obtained by UV irradiation ($\lambda \geq 300$ nm).

Introduction

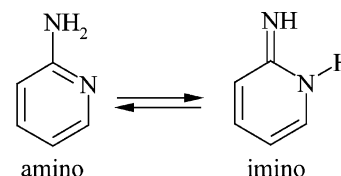
Tautomerism has an important role in biological system and has been actively investigated by many researchers. For example, the origin of serious DNA mutation is regarded as keto–enol and/or amino–imino tautomerisms.^{1–4} One of the most famous keto–enol tautomerisms is the system between 2(1*H*)-pyridinone and 2-hydroxypyridine (Scheme 1), which is frequently used to be the simplest model for the DNA bases such as cytosine, thymine, and uracil. So far, several matrix-isolation infrared (IR) analyses have been reported on tautomerism.^{5–8} Especially, Nowak et al. have found a photoinduced tautomerism from keto to enol by UV irradiation⁸ and have extended the analyses to analogous compounds including cytosine⁹ and its derivatives.^{10–13} On the other hand, the system between 2-aminopyridine and 2(1*H*)-pyridinimine (Scheme 2) is one of the simplest models for the amino–imino tautomerism which exists in the DNA bases such as cytosine, adenine, and guanine.^{1,3,4,14,15} However, only a few amino–imino tautomerisms have been investigated by IR spectroscopy.^{16,17} Recently, we investigated photoreaction of 2-aminopyridine and found the photoinduced reversible amino ($\text{N}=\text{C}-\text{NH}_2$)–imino ($\text{NH}-\text{C}=\text{NH}$) tautomerism (Scheme 2); the amino tautomer changes to the imino tautomer by UV irradiation ($340 > \lambda \geq 300$ nm) and the reverse change occurs by longer-wavelength light irradiation ($370 > \lambda \geq 340$ nm).¹⁷

In the present study, we have investigated the photoreaction of 2-amino-5-methylpyridine (Figure 1) in a low-temperature argon matrix by IR spectroscopy with the aid of density functional theory (DFT) calculation. Methylation of DNA base is a serious substitute reaction in biological system. In addition, a methyl group often brings about the stabilization through hyperconjugation and participation in intramolecular proton transfer.^{18–25} In the photoreaction of 2-amino-5-methylpyridine,

SCHEME 1



SCHEME 2



we found that the photoinduced amino–imino tautomerism occurs by UV irradiation ($340 > \lambda \geq 300$ nm) and also obtained the IR spectra of 2-amino-5-methylpyridine in the lowest electronic excited triplet (T_1) state and 5-methyl-2-pyridinamino radical which is produced by one hydrogen-atom dissociation. The photoinduced reversible amino–imino tautomerism mechanism is discussed on the basis of the experimental and theoretical results.

Experimental and Calculation Methods

2-Amino-5-methylpyridine was obtained from Wako Pure Chemical Industries. The gas mixture was prepared by passing argon gas (Nippon Sanso, 99.9999%) through the glass tube containing with sample in a vacuum line and was deposited onto a CsI plate cooled at 12 K by a closed-cycle helium refrigerator (Iwatani, CryoMini D510). The matrix temperature was monitored continuously by an Au–chromel thermocouple and was controlled by a thermostabilizer (Iwatani, TCU-4). Infrared (IR) absorption spectra were measured with an FTIR spectrophotometer (JASCO, FT/IR-615) equipped with an MCT detector, where accumulation was 100 times and the spectral

* Corresponding author. Tel: +81-82-424-5735. Fax: +81-82-424-5736. E-mail: rosso@hiroshima-u.ac.jp.

[†] Center for Quantum Life Sciences.

[‡] Department of Chemistry.

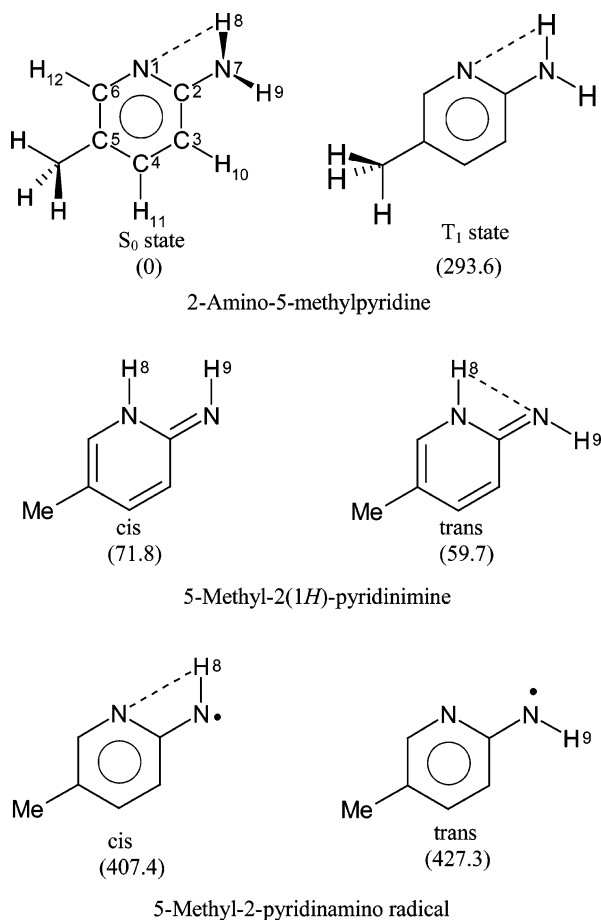


Figure 1. Structures of 2-amino-5-methylpyridine, 5-methyl-2(1H)-pyridinimine, and the 5-methyl-2-pyridinamino radical. Direction of methyl group for the imino tautomers and radicals is the same as that for the amino tautomer in the S_0 state. Relative energies (in kJ mol^{-1}) calculated at the B3LYP/6-31++G** level are given in parentheses, where the energy of one hydrogen atom is added in the values of the radicals.

resolution was 1 cm^{-1} . UV radiation from a superhigh-pressure mercury lamp (USHIO, SX-UI 501HQ) was used to induce photoreaction combined with a water filter to avoid thermal radiation and short-wavelength cutoff filters, Sigma UTF-30U ($\lambda \geq 300 \text{ nm}$), UTF-34U ($\lambda \geq 340 \text{ nm}$), SCF-37L ($\lambda \geq 370 \text{ nm}$), and SCF-42L ($\lambda \geq 420 \text{ nm}$) to isolate the desired wavelengths of radiation.

DFT calculations were performed using the Gaussian 03 program.²⁶ The density functional, B3LYP,^{27,28} with a basis set of 6-31++G** was used to estimate relative energies, optimized structures, and vibrational wavenumbers of conformers in the electronic ground (S_0) and T_1 states and radicals. Those in the first electronic excited singlet (S_1) state were calculated by the complete-active-space self-consistent-field (CASSCF) method with a basis set of 6-31G**. The active space used in the CASSCF calculations consists of 10 electrons and 8 active orbitals: the three π and three π^* orbitals on the pyridine ring, the amino nitrogen $2p_z$ and the pyridine nitrogen nonbonding electrons.

Results and Discussion

Optimized Structures. The structures and optimized geometrical parameters of 2-amino-5-methylpyridine, 5-methyl-2(1H)-pyridinimine, and 5-methyl-2-pyridinamino radical are summarized in Figure 1 and Table 1, respectively. Each bond

TABLE 1: Optimized Geometrical Parameters for 2-Amino-5-methylpyridine, 5-Methyl-2(1H)-pyridinimine, and 5-Methyl-2-pyridinamino Radical Calculated by the B3LYP/6-31++G Level**

parameter ^a	2-amino-5-methylpyridine		5-amino-2(1H)-pyridinimine		5-methyl-2-pyridin-amino radical	
	S_0	T_1	cis	trans	cis	trans
Bond Length/Å						
$d(1,2)$	1.339	1.310	1.407	1.401	1.378	1.376
$d(2,3)$	1.411	1.484	1.455	1.456	1.433	1.437
$d(3,4)$	1.387	1.430	1.360	1.363	1.381	1.382
$d(4,5)$	1.406	1.370	1.443	1.439	1.408	1.406
$d(5,6)$	1.396	1.488	1.361	1.365	1.417	1.418
$d(1,6)$	1.341	1.374	1.378	1.368	1.322	1.319
$d(2,7)$	1.387	1.358	1.294	1.294	1.333	1.337
$d(5,\text{Me})$	1.509	1.493	1.507	1.507	1.504	1.504
$d(3,10)$	1.086	1.084	1.084	1.085	1.084	1.087
$d(4,11)$	1.088	1.086	1.088	1.088	1.087	1.087
$d(6,12)$	1.089	1.084	1.085	1.084	1.090	1.091
$d(7,8)$	1.011	1.011		2.425	1.027	
$d(7,9)$	1.009	1.007	1.022	1.019		1.026
$d(1,8)$	2.434	2.476	1.011	1.012	2.348	
Bond Angle/deg						
$\angle(1,2,3)$	122.1	125.3	112.9	112.9	120.6	120.1
$\angle(2,3,4)$	118.4	116.8	122.0	121.7	119.6	120.0
$\angle(3,4,5)$	120.5	119.2	122.1	122.3	119.7	119.6
$\angle(4,5,6)$	115.9	119.2	116.3	116.1	116.8	116.6
$\angle(5,6,1)$	125.0	122.5	121.7	121.8	125.1	125.5
$\angle(6,1,2)$	118.1	117.0	125.0	125.3	118.1	118.3
$\angle(1,2,7)$	116.5	118.3	125.3	117.3	120.5	116.1
$\angle(4,5,\text{Me})$	122.2	123.4	121.2	121.4	122.0	122.1
$\angle(2,3,10)$	120.5	120.5	115.9	117.3	118.1	119.2
$\angle(3,4,11)$	119.6	120.2	119.3	119.2	120.4	120.3
$\angle(5,6,12)$	119.8	120.2	123.0	122.8	118.9	118.6
$\angle(2,7,8)$	114.2	118.5			107.3	
$\angle(2,7,9)$	117.4	121.9	112.3	110.5		108.8
$\angle(2,1,8)$			116.9	114.5		
$\angle(1,2,7,8)$	16.4	0.0	0.0	0.0	0.0	
$\angle(1,2,7,9)$	205.0	180.0	0.0	180.0		180.0

^a The values of other parameters are available upon request.

length of the amino and imino tautomers is the same as that of 2-aminopyridine and 2(1H)-pyridinimine within 0.01 \AA ($1 \text{ \AA} = 10^{-10} \text{ m}$),¹⁷ indicating no remarkable hyperconjugation of the methyl group with the pyridine ring geometrically. In the S_0 state of each tautomer and the radical, one hydrogen atom of the methyl group is planar and is directed to the C6 side in contrast to the hydrogen atom in the T_1 state of the amino tautomer which is directed to the C4 side (Figure 1). Hydrogen atoms of the amino group in the S_0 state are out of plane of the pyridine ring on the same side, whereas the hydrogen atom(s) of the amino group in the T_1 state and the imino group is planar to the ring. Most of the bond lengths for 5-methyl-2-pyridinamino radical have medium values between the amino and imino tautomers, except for the shortened C6–N1 and the lengthened C5–C6 bonds.

The C2–N7 bond is shortened for 2-amino-5-methylpyridine in the T_1 state and 5-methyl-2-pyridinamino radical and has considerable double bond character. For 2-amino-5-methylpyridine, the $\text{N1}\cdots\text{H8}$ distance ($d(1,8) = 2.434 \text{ \AA}$) is shorter than the sum of the van der Waals radii of H and N ($2.7 = 1.2 + 1.5 \text{ \AA}$), indicating the existence of the intramolecular $\text{NH}\cdots\text{N}$ hydrogen bond. For *trans*-5-methyl-2(1H)-pyridinimine, $d(1,8)$ is 1.012 \AA and $d(7,8)$ is 2.425 \AA , and for *cis*-5-methyl-2-pyridinamino radical, $d(7,8)$ is 1.027 \AA and $d(1,8)$ is 2.348 \AA . Thus, 2-amino-5-methylpyridine, the *trans*-5-methyl-2(1H)-pyridinimine, and *cis*-5-methyl-2-pyridinamino radical are stabilized by the intramolecular $\text{NH}\cdots\text{N}$ hydrogen bond. The hydrogen bond of the *cis* radical is the strongest among them.

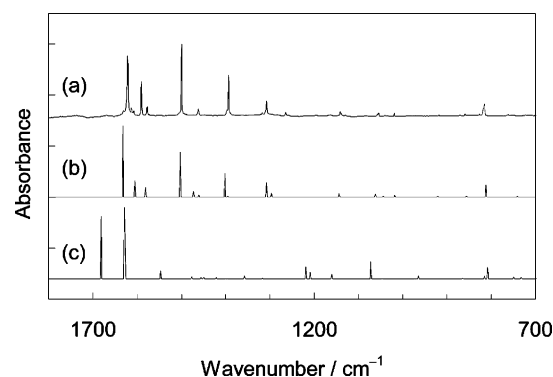


Figure 2. IR spectra of 2-amino-5-methylpyridine. (a) Matrix-isolated infrared spectrum. (b) and (c) Calculated spectrum of the amino and trans imino tautomers, respectively, by the B3LYP/6-31++G** level.

The DFT calculations show that the amino tautomer is more stable than the trans and cis imino conformers by 59.7 and 71.8 kJ mol⁻¹, respectively, which is similar to the results of 2-aminopyridine.¹⁷

IR Spectrum of 2-Amino-5-methylpyridine in the S₀ State.

An infrared spectrum of 2-amino-5-methylpyridine in an argon matrix is shown in Figure 2a, along with the calculated spectra of 2-amino-5-methylpyridine in the S₀ state (Figure 2b) and *trans*-5-methyl-2(1*H*)-pyridinimine being the most stable imino conformer (Figure 2c). The comparison of the observed spectrum with the calculated indicates that only the calculated amino spectrum reproduces satisfactorily the observed. This is consistent with the negligible imino population (<0.01%) estimated from the energy difference (59.7 kJ mol⁻¹) at the deposition temperature 298 K by the Boltzmann distribution law. Therefore, all the bands observed immediately after the deposition of the sample are assigned to the amino tautomer 2-amino-5-methylpyridine. Table 2 summarizes the observed and calculated wavenumbers.

IR Spectrum of 2-Amino-5-methylpyridine in the T₁ State.

After UV irradiation was stopped, the sample in the matrix at 12 K radiated blue phosphorescence for about 10 s, in analogy with the T₁ state of 2-aminopyridine.¹⁷ To observe photoinduced transient bands, we measured an infrared spectrum of the sample during UV irradiation ($\lambda \geq 300$ nm). The transient difference spectrum, which is obtained by subtracting the spectrum before UV irradiation from that during UV irradiation, is shown in Figure 3, together with the calculated spectrum of 2-amino-5-methylpyridine in the T₁ (upward) and S₀ (downward) states. The calculated spectrum reproduces satisfactorily the transient spectrum, indicating that the transient species is 2-amino-5-methylpyridine in the T₁ state. An intense band appearing at 1597 cm⁻¹ is assigned to the NH₂ bending vibration. The observed and calculated wavenumbers are summarized in Table 2, along with those of the S₀ state.

Almost all the geometrical changes between the S₀ and T₁ states of 2-amino-5-methylpyridine are the same as those of 2-aminopyridine within 0.01 Å except for the C5–C6 bond.¹⁷ The C5–C6 bond lengths of 2-amino-5-methylpyridine and 2-aminopyridine in the T₁ state are longer than those in the S₀ state by 0.092 and 0.078 Å, respectively.¹⁷

Identification of One Hydrogen-Atom Eliminated Intermediate, 5-Methyl-2-pyridinamino Radical. 2-Amino-5-methylpyridine is decomposed to several species by UV irradiation ($\lambda \geq 300$ nm). In the photolysis of *p*-toluidine, the 4-methyl-anilino radical is produced by UV irradiation ($\lambda \geq 300$ nm).²⁹ As such, a radical easily disappears by annealing, the radical can be distinguished from other photoproducts by annealing.^{29,30}

TABLE 2: Observed and Calculated Wavenumbers of 2-Amino-5-methylpyridine in the S₀ and T₁ States with Relative Intensities

S ₀ state				T ₁ state			
obs		calc ^a		obs		calc ^a	
ν/cm^{-1}	int	ν/cm^{-1}	int/km mol ⁻¹	ν/cm^{-1}	int	ν/cm^{-1}	int/km mol ⁻¹
3525	16.7	3629	12.7	3539	41.7	3670	19.0
3423	32.1	3510	15.4	3416	100	3524	44.4
3023	5.0	3128	7.2			3155	0.4
2990	2.4	3107	6.5	3063	10.0	3150	8.3
2958	2.9	3090	15.3	3044	1.8	3122	3.1
2936	3.0	3050	7.5	2984	3.2	3059	9.4
2908	0.7	3020	9.2	2924	3.0	2982	7.3
2877	1.4	2969	22.5	2897	3.3	2943	10.7
1621	83.8	1632	100	1597	87.2	1614	100
1591	47.5	1605	23.6	1556	6.7	1570	13.7
1577	12.6	1581	14.2	1523	4.2	1540	14.8
1500	100.0	1502	63.2	1438	2.5	1447	3.8
1462 ^b	7.7	1472	7.6			1434	3.5
		1461	3.1	1421	5.8	1418	10.7
1393	57.0	1402	33.0	1369	8.0	1378	2.6
		1395	1.5			1366	0.7
		1327	0.1	1296	19.2	1306	17.7
1308	19.7	1308	20.3	1278	16.7	1286	12.6
1265	4.3	1297	6.2			1206	1.7
		1222	0.1	1179	8.2	1190	7.0
1142	4.7	1144	5.2	1045	1.1	1049	5.0
1055	3.3	1062	4.2			1007	1.4
1041	0.3	1044	1.2	992	1.9	994	1.9
1019	3.2	1018	2.5			983	0.9
982	0.0	982	0.4			869	16.4
975	0.0	958	0.0	801	5.7	804	6.5
918	1.4	921	1.0	790	7.5	791	4.8
859	2.4	856	1.0			728	2.7
815 ^b	16.2	812	17.8			644	6.2
763	1.0	748	0.6			584	0.5
723	0.6	741	1.0			553	2.8
		647	0.9			483	0.0
		549	54.2			445	0.8
		491	67.9			396	1.5
		477	23.0			376	41.0
		417	0.5			300	0.3
		414	1.1			292	1.6
		354	21.7			257	0.6
		310	1.9			241	3.1
		292	1.2			165	1.1
		134	2.1			52	18.3
		71	0.1			23	28.2

^a Calculated at the B3LYP/6-31++G** level. The calculated wavenumbers are adjusted by a scaling factor of 0.98. ^b The bands exhibit splitting.

It is likely that the photolysis of 2-amino-5-methylpyridine also yields an analogous radical, 5-methyl-2-pyridinamino radical (Figure 1).

Figure 4a shows a difference spectrum, where the spectrum observed immediately after UV irradiation ($\lambda \geq 300$ nm) is subtracted from that after subsequent annealing at 28 K. The candidate radical has *cis* and *trans* conformations around the imino group (Figure 1), whose calculated spectra are shown in Figure 4b,c, respectively. The calculated spectrum of Figure 4b reproduces satisfactorily the downward bands in Figure 4a, which indicates that the downward bands are associated with *cis*-5-methyl-2-pyridinamino radical that is retained by the strong intramolecular NH \cdots N hydrogen bond. Thus, this radical is produced by the elimination of the H9 atom and might be stabilized by the methyl substituent, because the radical has been detected in a similar condition for *p*-toluidine²⁸ but is not detected for 2-aminopyridine.¹⁶ The radical was produced by UV irradiation ($\lambda \geq 300$ nm), but not longer-light irradiation ($\lambda \geq 340$ nm). The observed and calculated wavenumbers are summarized in Table 3, along with their relative band intensities

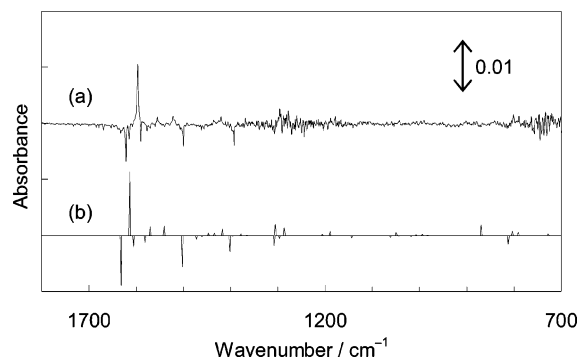


Figure 3. Photoinduced transient IR spectrum of 2-amino-5-methylpyridine in the T_1 state. (a) Observed difference spectrum, where the spectrum obtained immediately after the deposition of the sample is subtracted from that measured during UV irradiation ($\lambda \geq 300$ nm). (b) Calculated spectrum of 2-amino-5-methylpyridine in the T_1 (upward) and S_0 (downward) states, by the B3LYP/6-31++G** level.

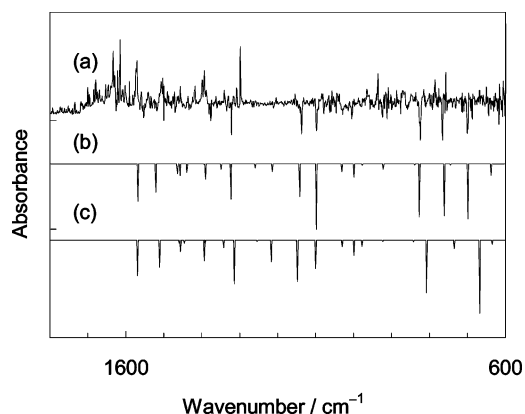


Figure 4. Difference IR spectrum of 5-methyl-2-pyridinamino radical (downward). (a) Observed spectrum, where the spectrum obtained immediately after UV irradiation ($\lambda \geq 300$ nm for 2 min) is subtracted from that after subsequent annealing at 28 K. (b) and (c) Calculated spectra of *cis*- and *trans*-5-methyl-2-pyridinamino radicals, respectively, by the B3LYP/6-31++G** level.

and assignments. The infrared spectrum of *cis*-5-methyl-2-pyridinamino radical is reported for the first time to our knowledge.

Identification of the Imino Tautomer, 5-Methyl-2(1H)-pyridinimine. Photolysis of 2-amino-5-methylpyridine in the matrix produced several stable photoproducts that can be distinguishable to each other by irradiation of different wavelengths. Figure 5a shows the difference spectrum, where the spectrum measured immediately after the first UV irradiation ($\lambda \geq 300$ nm) is subtracted from that after the second light irradiation ($\lambda > 370$ nm). The bands increasing in intensity by the second light irradiation (upward) were due to not only the parent species, 2-amino-5-methylpyridine, but also other photoproducts. The reverse change to produce 2-amino-5-methylpyridine suggests the existence of similar amino–imino tautomerism occurring in 2-aminopyridine.¹⁷ The imino tautomer, 5-methyl-2(1H)-pyridinimine, has two conformations (Figure 1). Several downward bands are assigned to the *trans* or *cis* conformer by comparing the observed spectrum with the calculated of the *trans* and *cis* conformers (Figure 5b,c). For example, the bands observed at 1671, 1615, 1541, 1158, and 1083 cm^{-1} are consistently associated with the *trans* conformer and the bands at 1679, 1633, 1571, 1298, 1154, and 1077 cm^{-1} , the *cis* conformer. Therefore, one of the stable photoproducts is surely identified as 5-methyl-2(1H)-pyridinimine. The *trans* imino conformer is produced by the H8 atom migration, which

TABLE 3: Observed and Calculated Wavenumbers of *cis*-5-Methyl-2-pyridinamino Radical

obs		calc ^a		assignment ^b
ν/cm^{-1}	int	ν/cm^{-1}	int/km mol ⁻¹	
3417	37.8	3372	9.3	$\nu(\text{NH})$
		3158	5.2	
		3117	24.0	
		3083	69.9	
		3061	27.5	
		3024	25.3	
		2972	46.4	
1553	19.0	1568	57.0	$\nu(\text{CC}) + \nu(\text{CN})$
1519	21.6	1521	43.0	$\nu(\text{CC})$
		1464	14.7	
1470	18.9	1457	18.0	Me def
		1439	13.2	
		1393	1.1	
1376	32.4	1390	23.6	$\beta(\text{ring}, \text{NH}, \text{CH})$
		1349	8.2	
1322	64.9	1323	53.6	$\beta(\text{CH}, \text{NH})$
		1259	5.9	
1213	13.5	1214	12.2	$\nu(\text{C-Me}) + \beta(\text{CH})$
1137	75.7	1142	50.0	$\beta(\text{CH}, \text{NH})$
1098	70.3	1098	100	$\beta(\text{CH}, \text{NH})$
1029	16.2	1031	11.7	$\gamma(\text{C-Me})$
1005	21.6	999	20.1	$\beta(\text{CH}, \text{Me})$
		977	1.8	
		970	0.0	
925	27.0	922	7.7	$\gamma(\text{CH}, \text{Me})$
		839	1.3	
834	97.3	827	81.2	$\gamma(\text{ring}, \text{CH})$
766	100	761	79.2	$\gamma(\text{CH}, \text{NH})$
		745	1.4	
701	91.9	699	84.1	$\gamma(\text{CH}, \text{NH})$
		638	17.3	
		491	18.8	
		477	2.8	
		433	18.7	
		385	0.4	
		305	0.7	
		294	0.5	
		122	0.0	
		40	0.2	

^a Calculated at the B3LYP/6-31++G** level. The calculated wavenumbers are adjusted by a scaling factor of 0.98. ^b ν , stretching; β , in-plane deformation mode; γ , out-of-plane deformation mode.

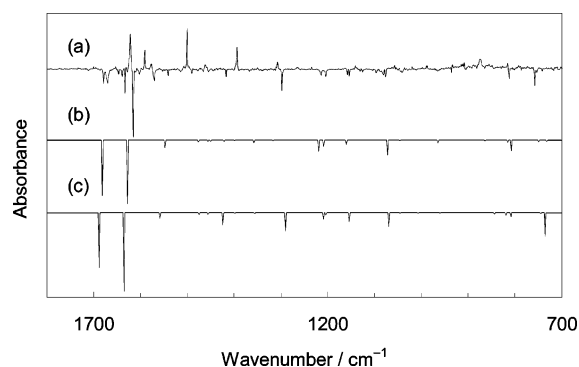


Figure 5. Difference IR spectrum of 5-methyl-2(1H)-pyridinimine (downward), where most of the upward bands are due to 2-amino-5-methylpyridine. (a) Observed spectrum, where the spectrum obtained immediately after the first UV irradiation ($\lambda \geq 300$ nm for 5 min) is subtracted from that after the second light irradiation ($\lambda \geq 340$ nm for 5 min). (b) and (c) Calculated spectra of *trans*- and *cis*-5-methyl-2(1H)-pyridinimine, respectively, by the B3LYP/6-31++G** level.

is assisted by the N7H8...N1 hydrogen bond, and then transformed into the *cis* imino conformer by UV irradiation. The observed and calculated wavenumbers are summarized in Table 4, along with their relative intensities.

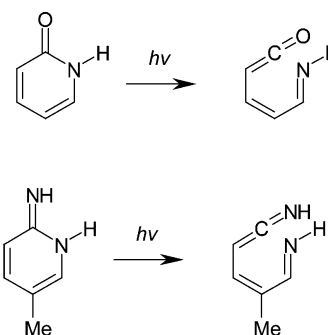
TABLE 4: Observed and Calculated Wavenumbers of 5-Methyl-2(1*H*)-pyridinimine

obs		calc ^a			
<i>v</i> /cm ⁻¹	int	trans		cis	
		<i>v</i> /cm ⁻¹	int/km mol ⁻¹	<i>v</i> /cm ⁻¹	int/km mol ⁻¹
3456	6.4			3551	10.6
3447	17.8	3542	17.5		
3351	2.6	3455	2.7		
				3398	3.7
		3147	1.6	3165	0.5
		3141	2.9	3145	2.6
		3106	4.1	3112	4.1
		3049	6.1	3050	6.3
		3013	6.7	3014	6.5
		2965	18.8	2966	17.8
1679	17.9			1689	70.4
1671	17.5	1682	88.0		
1633 ^b	32.8			1635	100
1615	100	1628	100		
1571	16.0			1558	7.0
1541	7.2	1548	11.6		
1490	5.0	1476	3.1	1475	2.5
		1456	2.2	1456	2.2
		1450	1.9	1444	0.1
1417	11.5	1422	2.3	1424	15.2
		1399	0.4	1398	0.6
		1358	4.3	1356	1.0
		1317	0.9		
1298	32.4			1290	23.5
1215	5.7	1219	17.3	1209	8.2
1205	8.5	1209	9.6	1204	3.0
1158	8.7	1160	6.9		
1154	10.7			1154	11.5
1083	2.8	1072	23.8		
1077	8.3			1069	17.5
		1046	0.5	1046	0.5
		1006	0.1	1007	0.9
		971	0.0	982	0.0
936	5.4	965	4.3	960	0.3
		864	1.1	844	1.8
		816	3.6	819	3.3
812	14.3	808	16.6	809	4.9
758	25.1	749	2.4	745	1.1
755	2.6	732	2.3	736	30.1
		697	2.2	691	2.1
		637	26.1	635	0.3
		635	0.1	565	2.0
		468	3.4	463	0.6
		465	14.1	460	25.4
		431	0.9	436	6.3
		379	0.9	374	0.0
		292	0.3	293	0.4
		266	1.0	270	0.3
		139	0.0	148	0.1
		104	0.3	104	0.2

^a Calculated at the B3LYP/6-31++G** level. The calculated wavenumbers are adjusted by a scaling factor of 0.98. ^b The band exhibits splitting.

The DFT calculation predicts that the trans imino conformer with the intramolecular NH...N hydrogen bond is more stable than the cis conformer by 12.1 kJ mol⁻¹ and that the barrier height from the trans to the cis conformer is 94.0 kJ mol⁻¹. It is well-known that the conformational change around the imino group often occurs by UV irradiation;^{29–34} the two conformers in imino-oxo methylcytosine change each other by UV irradiation.³¹ Then, we attempted to separate the two conformers of 5-methyl-2(1*H*)-pyridinimine, but no remarkable selective population change was detected by irradiation of different wavelengths in the present study. No conformational change between trans and cis of imino tautomer were also observed in 2-aminopyridine.¹⁷

Other Photoproducts. Nowak et al. have reported the photolysis from 2(1*H*)-pyridinone to a conjugated ketene compound (Scheme 3).⁸ In 5-methyl-2(1*H*)-pyridinimine, a

SCHEME 3**TABLE 5: Relative Energies and C=C=NH Conjugated Stretching Wavenumbers of Conformers for Kettenimine, 4-Methyl-1,3-pentadien-1,5-diimine**

conformer	relative energy/kJ mol ⁻¹ ^a	<i>v</i> /cm ⁻¹ ^b
<i>tttt</i>	0	2063
<i>tttc</i>	6.8	2065
<i>ttct</i>	14.8	2062
<i>tcct</i>	9.0	2063
<i>cttt</i>	10.3	2053
<i>ttcc</i>	22.2	2065
<i>tcct</i>	12.4	2056
<i>ccct</i>	19.9	2058
<i>tctc</i>	14.1	2065
<i>ctct</i>	24.4	2051
<i>cttc</i>	17.7	2058
<i>tecc</i>	27.0	2063
<i>ctcc</i>	30.6	2056
<i>cctc</i>	27.0	2062
<i>ccct</i>	29.9	2035
<i>cccc</i>	41.2	2057

^a Calculated at the B3LYP/6-31++G** level. ^b The wavenumbers are adjusted by a scaling factor of 0.98.

similar ring opening to produce ketenimine, 4-methyl-1,3-pentadien-1,5-diimine, might occur (Scheme 3). The N1–C2 bond of the cis imino 5-methyl-2(1*H*)-pyridinimine is longer by 0.006 Å than that of the trans imino conformer stabilized by the intramolecular N1H8...N7 hydrogen bond. In addition, reaction barrier from the cis imino to the ketenimine is lower than that from the trans imino by about 15.5 kJ mol⁻¹. Thus, the photoreaction to ketenimine by cleavage of the N1–C2 bond mainly occurs in the cis imino conformer.

The ketenimine has 16 conformations around four rotational axes HNCC–C=C–C=NH; for example, the ketenimine in Scheme 3 is represented as the *ccct* (cis–cis–cis–trans) conformer. The *ccct* conformer is produced by the ring opening of 5-methyl-2(1*H*)-pyridinimine directly but is less stable by about 30 kJ mol⁻¹ than the most stable conformer *tttt* in Table 5. The ketenimine has a characteristic C=C=NH conjugated stretching band appearing in the 2030–2060 cm⁻¹ region. The calculated wavenumber of the C=C=NH conjugated stretching for each conformer is shown in Table 5, together with its relative energy. Figure 6 shows the time dependence of UV irradiation ($\lambda \geq 300$ nm) of the IR spectra. In the C=C=NH conjugated stretching region, the 2020 cm⁻¹ band appears in early irradiation period, and the 2047 cm⁻¹ band increases in longer irradiation time compared to the former. The *ccct* conformer has the lowest calculated wavenumber at 2035 cm⁻¹, which is away from the others. Thus, the 2020 cm⁻¹ band is associated with the *ccct* conformer and the 2047 cm⁻¹ bands is related to the more stable conformers such as the *tttt* conformer produced by photoinduced rotation. On the other hand, the intense band at 2155 cm⁻¹ is assigned to the C≡C stretching of some photodecomposed product that is likely to be produced by the photolysis of the ketenimine.

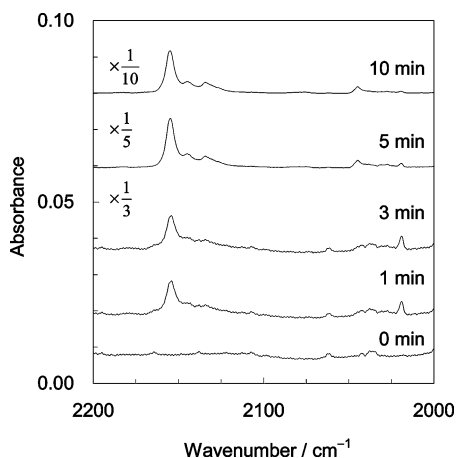


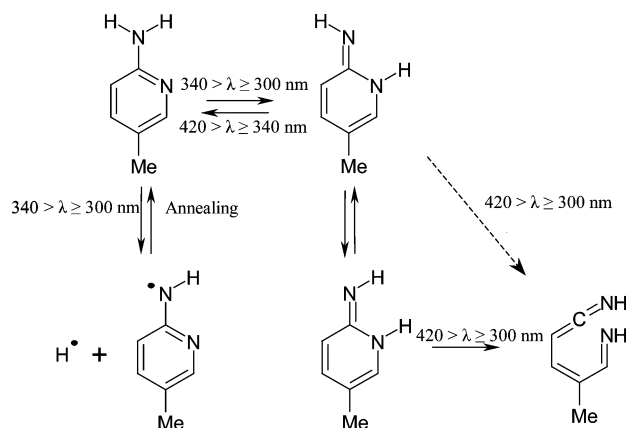
Figure 6. IR spectra of 2-amino-5-methylpyridine at different times of light irradiation ($\lambda \geq 300$ nm) in the 2000–2200 cm^{-1} region.

Photoreaction Mechanism of 2-Amino-5-methylpyridine and Amino–Imino Tautomerism. The amino–imino tautomerism between 2-amino-5-methylpyridine and 5-methyl-2(1*H*)-pyridinimine is found in the present study. The amino tautomer, 2-amino-5-methylpyridine, changes to the imino tautomer, 5-methyl-2(1*H*)-pyridinimine, by UV irradiation ($340 > \lambda \geq 300$ nm), and the reverse change occurs by longer-wavelength light irradiation ($420 > \lambda \geq 340$ nm). The DFT calculation leads that 2-amino-5-methylpyridine is more stable than *trans*- and *cis*-5-methyl-2(1*H*)-pyridinimine by 59.7 and 71.8 kJ mol^{-1} , respectively, and the barrier height from 2-amino-5-methylpyridine to *trans*-5-methyl-2(1*H*)-pyridinimine is 205.7 kJ mol^{-1} . The barrier height from the *trans* to the *cis* imine conformer is 94 kJ mol^{-1} . These barrier heights are high enough to avoid thermal conversion of structures in the matrix at 12 K.

Dissociation energy of N–H bond to produce *cis*-5-methyl-2-pyridinamino radical and H atom is calculated to be 407.4 kJ mol^{-1} , which is nearly consistent with the first irradiation energy (300 nm \approx 400 kJ mol^{-1}). The intensities of bands assigned to the 5-methyl-2-pyridinamino radical are much weaker than those of the other photoproducts. This means that the hydrogen-atom migration from the amino to imino tautomer is easier than the hydrogen-atom dissociation to produce the radical in photoreaction process of 2-amino-5-methylpyridine. On the other hand, *trans*-5-methyl-2-pyridinamino radical is not observed, suggesting that the hydrogen-bonded H8 atom of 2-amino-5-methylpyridine is not released but is migrated from N7 to N1 atom by UV irradiation. Thus, the imine has been produced by this migration for 2-amino-5-methylpyridine as well as 2-aminopyridine produced no radical intermediates by UV irradiation.¹⁷ It is therefore noted that the amino–imino tautomerism through the hydrogen-atom migration assisted by the intramolecular $\text{NH}\cdots\text{N}$ hydrogen bond can easily proceed without the methyl substituent, though the amino–imino tautomerism through the radical intermediate stabilized by the methyl substituent is also possible in *p*-toluidine.²⁹ Then, the photoreaction mechanism of 2-amino-5-methylpyridine in the present study is shown in Scheme 4.

Intramolecular proton (or hydrogen-atom) migrations often occur in low-temperature matrixes by tunneling effect. Rostkowska et al. have recently reported that a tautomerism from thione to thiol in thiourea occurs by UV irradiation, in analogy with the photoinduced keto–enol tautomerism, and the reverse change occurs by tunneling effect.^{35–37} In 2-amino-5-methylpyridine, no change from the imino to amino tautomer occurs in the matrix in darkness at least for 3 h. Then, the tunneling

SCHEME 4



tautomerism mechanism in this system is ruled out and the tautomerism occurs through electronic excited states.

Schematic potential energies for the tautomerism are shown in Figure 7, where the energies of the stable and transition structures in the S_0 and T_1 states are calculated by the DFT method, whereas those in the S_1 state are obtained by the CASSCF(10,8) method and the vertical transition energies from the stable S_0 to S_1 states are obtained by the time-dependent DFT method. The first irradiation wavelength ($340 > \lambda \geq 300$ nm) is consistent with the S_1 – S_0 transition energy of the amino tautomer and the second irradiation ($420 > \lambda \geq 340$ nm) is consistent with that of the imino tautomer as well as 2-aminopyridine.¹⁷ The tautomerism might proceed in the S_1 state because the molecular orbital phases at LUMO of the imino tautomer are consistent with those of the amino tautomer (Figure 8). However, the energy of the first irradiation is not enough to get over the barrier from the amino to imino tautomer in the S_1 state; the amino tautomer is less stable than the imino by 69.4 kJ mol^{-1} and the tautomerism barrier height from the amino to imino is 164.6 kJ mol^{-1} , which denotes the same tendency of keto–enol tautomerism between 2(1*H*)-pyridinone and 2-hydroxypyridine.^{38–41} On the other hand, the DFT calculations show that in the T_1 state the *trans* imino tautomer is more stable than the amino tautomer by 30.4 kJ mol^{-1} and the tautomerism barrier from the amino to imino tautomer is 154.7 kJ mol^{-1} .

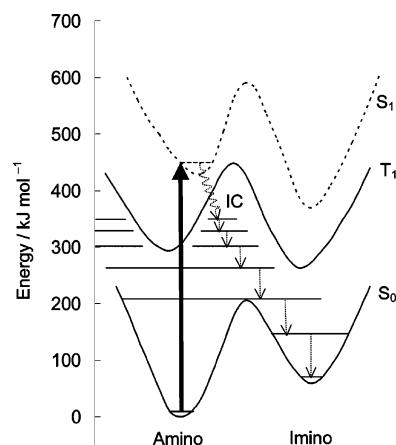


Figure 7. Schematic potential energy surfaces for amino–imino tautomerism between 2-amino-5-methylpyridine and 5-methyl-2(1*H*)-pyridinimine. Optimized minima in the S_0 and T_1 states (solid line) are obtained by the B3LYP/6-31++G** level, whereas those in the S_1 state (broken line) are obtained by the CASSCF(10,8)/6-31G** level. The vertical transition energies from the S_0 to S_1 states are calculated at the time-dependent B3LYP/6-31++G** level. Dotted lines with arrows represent vibrational relaxation process.

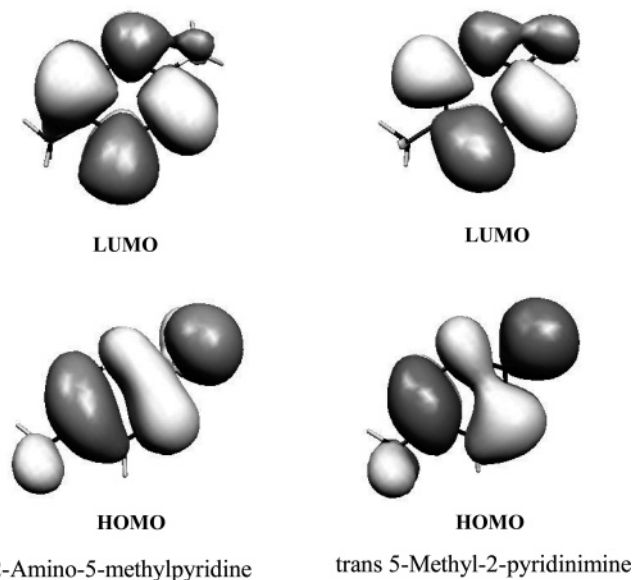


Figure 8. Molecular orbital phases at HOMO and LUMO of 2-amino-5-methylpyridine and *trans*-5-methyl-2(1*H*)-pyridinimine. The orbitals shown are on $|\Psi| = 0.015$ surface.

The barrier height in the T_1 state is $448.3 \text{ kJ mol}^{-1}$ from the potential minimum in the S_0 state of the amino and is higher than the first excitation energy ($300 \text{ nm} \approx 400 \text{ kJ mol}^{-1}$). Then, it seems unlikely that the photoinduced tautomerism proceeds on the S_1 or T_1 potential energy surface. The tautomerism occurs in vibrational relaxation at the excited vibrational levels of the S_0 state after the internal conversion from the S_1 (or T_1) to the S_0 state, as shown in Figure 7. The reverse tautomerism mechanism also proceeds in vibrational relaxation process; the second irradiation excites only the imino tautomer to its S_1 state, which immediately changes into the S_0 states of the imino and amino tautomers through the vibrational relaxation. Because the amino tautomer is not excited by the second irradiation, the imino gradually turns to the amino.

Conclusion

Photoinduced reversible tautomerism between 2-amino-5-methylpyridine and 5-methyl-2(1*H*)-pyridinimine has been found by matrix-isolation infrared spectroscopy and DFT calculation. The amino tautomer is more stable and changes into the imino upon UV irradiation ($340 > \lambda \geq 300 \text{ nm}$). The tautomerism occurs in vibrational relaxation process from electronic excited state to the ground state, because the UV excitation energy is approximately comparable to the S_1 – S_0 transition energy and is lower than the tautomerism barriers in the S_1 and T_1 states. In the UV irradiation for the amino tautomer, the tautomerism being a proton (hydrogen atom) migration assisted by the intramolecular hydrogen bond proceeds, whereas the non-hydrogen bonded hydrogen-atom dissociation produces a 5-methyl-2-pyridinamino radical that reverts to the initial amino tautomer by annealing procedure at 28 K. The reverse tautomerism from the imino to amino tautomer accompanying the ring cleavage of the imino to produce the ketenimine compound occurs by longer-wavelength light irradiation ($420 > \lambda \geq 340 \text{ nm}$). In addition, a photoinduced transient species was found during the UV excitation and was identified as the amino tautomer in the T_1 state.

Acknowledgment. This study was partly supported by grants from the Ministry of Education, Culture, Sports, Science, and Technology of Japan.

References and Notes

- Rueda, M.; Luque, F. J.; López, J. M.; Orozco, M. *J. Phys. Chem. A* **2001**, *105*, 6575.
- Fogarasi, G. *J. Phys. Chem. A* **2002**, *106*, 1381.
- Salter, L. M.; Chaban, G. M. *J. Phys. Chem. A* **2002**, *106*, 4251.
- Crespo-Hernández, C. E.; Cohen, B.; Hare, P. M.; Kohler, B. *Chem. Rev.* **2004**, *104*, 1977.
- Smets, J.; Maes, G. *Chem. Phys. Lett.* **1991**, *187*, 532.
- Lapinski, L.; Nowak, M. J.; Fulara, J.; Les, A.; Adamowicz, L. *J. Phys. Chem.* **1992**, *96*, 6250.
- Dkhissi, A.; Houben, L.; Smets, J.; Adamowicz, L.; Maes, G. *J. Mol. Struct.* **1999**, *484*, 215.
- Nowak, M. J.; Lapinski, L.; Fulara, J.; Les, A.; Adamowicz, L. *J. Phys. Chem.* **1992**, *96*, 1562.
- Nowak, M. J.; Lapinski, L.; Fulara, J. *Spectrochim. Acta A* **1989**, *45*, 229.
- Lapinski, L.; Nowak, M. J.; Fulara, J.; Les, A.; Adamowicz, L. *J. Phys. Chem.* **1990**, *94*, 6555.
- Nowak, M. J.; Lapinski, L.; Rostkowska, H.; Les, A.; Adamowicz, L. *J. Phys. Chem.* **1990**, *94*, 7406.
- Vranken, H.; Smets, J.; Maes, G.; Lapinski, L.; Nowak, M. J.; Adamowicz, L. *Spectrochim. Acta A* **1994**, *50*, 875.
- Lapinski, L.; Nowak, M. J.; Kwiatkowski, J. S.; Leszczynski, J. *J. Phys. Chem. A* **1999**, *103*, 280.
- Hanus, M.; Kabeláč, M.; Rejnek, J.; Ryjáček, F.; Hobza, P. *J. Phys. Chem. B* **2004**, *108*, 2087.
- Tomić, K.; Tatchen, J.; Marian, C. M. *J. Phys. Chem. A* **2005**, *109*, 8410.
- Abdulla, H. I.; El-Bermani, M. F. *Spectrochim. Acta A* **2001**, *57*, 2659.
- Akai, N.; Ohno, K.; Aida, M. *Chem. Phys. Lett.* **2005**, *413*, 306.
- Li, X.; Eriksson, L. A. *Chem. Phys. Lett.* **2005**, *401*, 99.
- Radisic, D.; Bowen, K. H., Jr.; Dabkowska, I.; Storoniak, P.; Rak, J.; Gutowski, M. *J. Am. Chem. Soc.* **2005**, *127*, 6443.
- Nishi, K.; Sekiya, H.; Kawakami, H.; Mori, A.; Nishimura, Y. *J. Chem. Phys.* **1999**, *111*, 3961.
- Vendrell, O.; Moreno, M.; Lluch, J. M. *J. Chem. Phys.* **2002**, *117*, 7525.
- Ushiyama, H.; Takatsuka, K. *Angew. Chem., Int. Ed.* **2005**, *44*, 1237.
- Mulliken, R. S.; Rieke, C. A.; Brown, W. G. *J. Am. Chem. Soc.* **1941**, *63*, 41.
- Ehrens, S. *J. Am. Chem. Soc.* **1961**, *83*, 4493.
- Flurry, R. L., Jr.; Lykos, P. G. *J. Am. Chem. Soc.* **1963**, *85*, 1033.
- Frisch, M. J.; Trucks, G. W.; Schlegel, H. B.; Scuseria, G. E.; Robb, M. A.; Cheeseman, J. R.; Montgomery, Jr., J. A.; Vreven, T.; Kudin, K. N.; Burant, J. C.; Millam, J. M.; Iyengar, S. S.; Tomasi, J.; Barone, V.; Mennucci, B.; Cossi, M.; Scalmani, G.; Rega, N.; Petersson, G. A.; Nakatsuji, H.; Hada, M.; Ehara, M.; Toyota, K.; Fukuda, R.; Hasegawa, J.; Ishida, M.; Nakajima, T.; Honda, Y.; Kitao, O.; Nakai, H.; Klene, M.; Li, X.; Knox, J. E.; Hratchian, H. P.; Cross, J. B.; Bakken, V.; Adamo, C.; Jaramillo, J.; Gomperts, R.; Stratmann, R. E.; Yazyev, O.; Austin, A. J.; Cammi, R.; Pomelli, C.; Ochterski, J. W.; Ayala, P. Y.; Morokuma, K.; Voth, G. A.; Salvador, P.; Dannenberg, J. J.; Zakrzewski, V. G.; Dapprich, S.; Daniels, A. D.; Strain, M. C.; Farkas, O.; Malick, D. K.; Rabuck, A. D.; Raghavachari, K.; Foresman, J. B.; Ortiz, J. V.; Cui, Q.; Baboul, A. G.; Clifford, S.; Cioslowski, J.; Stefanov, B. B.; Liu, G.; Liashenko, A.; Piskorz, P.; Komaromi, I.; Martin, R. L.; Fox, D. J.; Keith, T.; Al-Laham, M. A.; Peng, C. Y.; Nanayakkara, A.; Challacombe, M.; Gill, P. M. W.; Johnson, B.; Chen, W.; Wong, M. W.; Gonzalez, C.; Pople, J. A. *Gaussian 03*, revision B.5; Gaussian, Inc.: Wallingford, CT, 2003.
- Becke, A. D. *J. Chem. Phys.* **1993**, *98*, 5648.
- Lee, C.; Yang, W.; Parr, R. G. *Phys. Rev. B* **1988**, *37*, 785.
- Akai, N.; Yoshida, H.; Ohno, K.; Aida, M. *Chem. Phys. Lett.* **2005**, *403*, 390.
- Akai, N.; Kudoh, S.; Nakata, M. *J. Phys. Chem. A* **2003**, *107*, 6725.
- Szczesniak, M.; Leszczyński, J.; Person, W. B. *J. Am. Chem. Soc.* **1992**, *114*, 2731.
- Ujike, K.; Kudoh, S.; Nakata, M. *Chem. Phys. Lett.* **2004**, *396*, 288.
- Ujike, K.; Akai, N.; Kudoh, S.; Nakata, M. *J. Mol. Struct.* **2005**, *735/736*, 335.
- Ujike, K.; Kudoh, S.; Nakata, M. *Chem. Phys. Lett.* **2005**, *409*, 52.
- Rostkowska, H.; Lapinski, L.; Khvorostov, A.; Nowak, M. J. *J. Phys. Chem. A* **2003**, *107*, 6373.
- Rostkowska, H.; Lapinski, L.; Khvorostov, A.; Nowak, M. J. *Chem. Phys.* **2004**, *298*, 223.
- Lapinski, L.; Rostkowska, H.; Khvorostov, A.; Yaman, M.; Fausto, R.; Nowak, M. J. *J. Phys. Chem. A* **2004**, *108*, 5551.
- Sobolewski, A. L. *Chem. Phys. Lett.* **1993**, *211*, 293.
- Barone, V.; Adamo, C. *Chem. Phys. Lett.* **1994**, *226*, 399.
- Sobolewski, A. L.; Adamowicz, L. *Chem. Phys.* **1996**, *213*, 193.
- Sobolewski, A. L.; Adamowicz, L. *J. Phys. Chem.* **1996**, *100*, 3933.